STUDIES OF LOCALIZED SPACE-CHARGE WAVES IN SPACE-CHARGE DOMINATED BEAMS[*]

J. G. Wang and M. Reiser

Institute for Plasma Research, University of Maryland, College Park, MD 20742

The results of the experiments on localized space-charge waves are presented. This includes the generation and propagation of space-charge waves in coasting beams, the end effect on space-charge waves in bunched beams, and the application of localized space-charge waves to beam diagnostics.

I. INTRODUCTION

Space-charge waves are an important subject in the study of charged particle beams [1,2]. They have wide applications in microwave and free-electron laser generation, in particle accelerators, and in plasmas. The topic has been studied extensively. Experiments and analyses are usually carried out with sinusoidal signals. In many applications like in particle accelerators, space-charge waves are often generated in the form of localized perturbations due to short time-scale disturbances. For understanding of beam physics, controlled experiments with localized space-charge waves would be useful.

We have studied space-charge waves in the form of localized perturbations in space-charge dominated electron beams. Three topics have been investigated, including the generation of space-charge waves, the measurement of the geometry factor g, and the effect of bunch ends on space-charge waves. These studies have led us to develop a new beam diagnostic technique.

Our experiments are performed in an electron beam transport facility consisting of a short-pulse electron beam injector and a five meter long periodic solenoid focusing channel. The key device in the injector is a gridded electron gun which is able to produce the desired beam parameters with localized perturbations. The beam is matched with three solenoids into the transport channel consisting of 36 short solenoid lenses with a period of 13.6 cm. The beam pipe has a radius of 1.9 cm and the beam radius is less than 1 cm depending on the beam current, energy and focusing conditions. The diagnostic tools along the channel include five fast wall-current monitors for non-destructive beam current measurement, and three beam energy analyzers for the time-resolved beam energy measurement. At the end of the channel a diagnostic chamber houses a beam transverse image identifier and a beam energy spectrometer. Typical beam parameters in the experiments are: beam energy of 2.5 keV to 5 keV, beam current of 30 mA to 70 mA, transverse effective emittance (4 x rms) of about 90 mm mrad, and pulse length of 30 to 70 ns. The beams are fully space-charge dominated.

II. GENERATION OF LOCALIZED SPACE-CHARGE WAVES

Conventionally, space-charge waves are generated in velocity modulation devices always in pairs, i.e. both slow wave and fast wave with almost the same amplitudes. We have demonstrated that with the introduction of a current modulation and strong enough space-charge effect, either a single slow wave or a single fast wave can been produced experimentally. Combinations of the two waves with different amplitude and polarity relations can also be generated. The experimental results are supported by a more complete time-domain analysis [3].

In our experiment the initial perturbation is introduced to the beam by modulating the rectangular cathode-grid pulse with a small bump. This corresponds to a positive velocity perturbation on the beam particles, which in turn produces the initial density, and current perturbations. The space-charge waves then propagate along the beam in the form of localized perturbations. The relative strength of the initial current, or density perturbation over the given velocity perturbation can vary over a wide range.

Figure 1 shows the beam current waveforms measured at two different locations along the transport channel. The slow and fast waves appearing in the beam current signals, are generated in almost equal amplitudes and opposite polarities. The two space-charge waves become more and more separate from each other with distance of propagation. This effect is what is usually discussed in the literature about generation and propagation of space-charge waves.
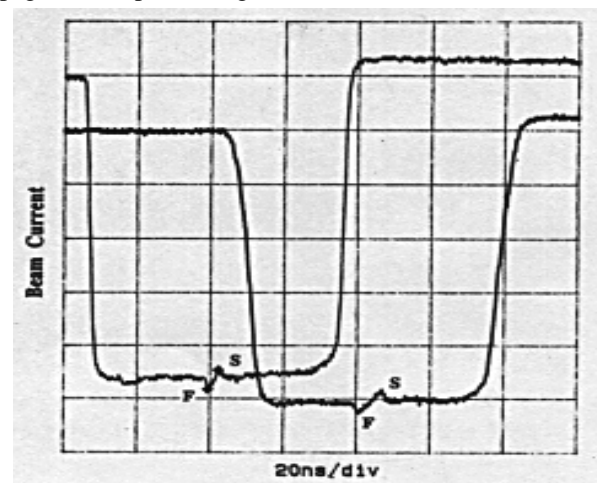

Fig. 1. Beam current waveforms with perturbations measured at the channel distances of s=0.624 m and s=3.48 m, respectively (s=0 is the cathode position), where F is for the fast wave and S is for the slow wave.

Figure 2 shows localized space-charge waves produced with initial perturbation conditions different from that in Fig. 1. Only one fast wave with a positive polarity has been generated on the electron beam current, which propagates toward the beam front. By contrast, Fig. 3 shows the beam

current waveforms with only one slow wave, which has a negative polarity and propagates toward the beam tail. Similar results are also obtained from the beam energy measurement. These new phenomena happen in a space-charge dominated beam and require specific, initial perturbation conditions on the beam parameters.
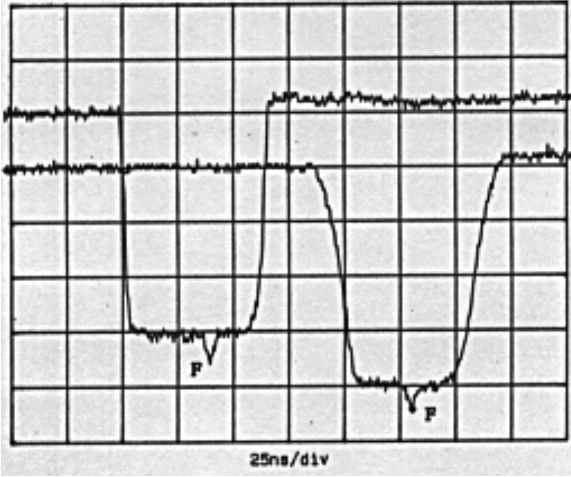

Fig. 2. Beam current waveforms with only one fast wave, taken at the same locations as that in Fig. 1.
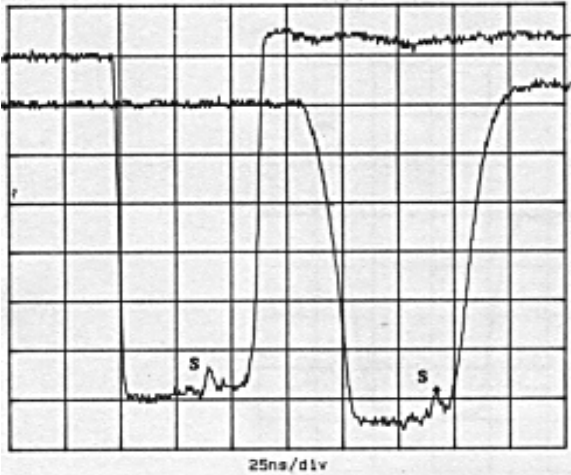

Fig. 3. Beam current waveforms with only one slow wave as measured at the same locations as that in Fig. 1.

An one-dimensional cold fluid model has been employed to investigate the generation of localized space-charge waves in time domain. The analysis shows that the perturbed beam line-charge density Λ_1, velocity v_1, and current i_1 are

$$\Lambda_1(z,t) = -\frac{\Lambda_0}{2}\left(\frac{v_{1i}}{c_s} - \frac{\Lambda_{1i}}{\Lambda_0}\right)h\left(t - \frac{z}{v_0 - c_s}\right) +$$
$$+ \frac{\Lambda_0}{2}\left(\frac{v_{1i}}{c_s} + \frac{\Lambda_{1i}}{\Lambda_0}\right)h\left(t - \frac{z}{v_0 + c_s}\right),$$

$$v_1(z,t) = +\frac{c_s}{2}\left(\frac{v_{1i}}{c_s} - \frac{\Lambda_{1i}}{\Lambda_0}\right)h\left(t - \frac{z}{v_0 - c_s}\right) +$$
$$+ \frac{c_s}{2}\left(\frac{v_{1i}}{c_s} + \frac{\Lambda_{1i}}{\Lambda_0}\right)h\left(t - \frac{z}{v_0 + c_s}\right),$$

$$i_1(z,t) = -\frac{i_0}{2}\left(1 - \frac{c_s}{v_0}\right)\left(\frac{v_{1i}}{c_s} - \frac{\Lambda_{1i}}{\Lambda_0}\right)h\left(t - \frac{z}{v_0 - c_s}\right) +$$
$$+ \frac{i_0}{2}\left(1 + \frac{c_s}{v_0}\right)\left(\frac{v_{1i}}{c_s} + \frac{\Lambda_{1i}}{\Lambda_0}\right)h\left(t - \frac{z}{v_0 + c_s}\right).$$

Here $h(t)$ is the perturbation waveform with an amplitude of unity, the subscripts 0 and 1i are for the unperturbed and initial perturbation amplitudes, respectively, and

$$c_s = \sqrt{\frac{eg\Lambda_0}{4\pi m\varepsilon_0 \gamma^5}} \tag{1}$$

is the speed of the waves in the beam frame, with g being a geometry factor described in next section. The condition for generating only one fast wave is

$$\frac{v_{1i}}{c_s} = \frac{\Lambda_{1i}}{\Lambda_0}, \quad \text{or} \quad \frac{i_{1i}}{i_0} = \left(1 + \frac{v_0}{c_s}\right)\frac{v_{1i}}{v_0}, \tag{2}$$

while the condition for producing only one slow wave is

$$\frac{v_{1i}}{c_s} = -\frac{\Lambda_{1i}}{\Lambda_0}, \quad \text{or} \quad \frac{i_{1i}}{i_0} = \left(1 - \frac{v_0}{c_s}\right)\frac{v_{1i}}{v_0}. \tag{3}$$

The wave velocity c_s is a measure for the effects of space charge in a beam. A beam with a large c_s reduces the required value of the relative current perturbation for a given relative velocity perturbation in a practical device. Thus Eqs. (2) and (3) can be more easily satisfied in a space-charge dominated beam.

III. MEASUREMENT OF GEOMETRY FACTOR

The geometry factor g is an important parameter in longitudinal beam dynamics, which relates the longitudinal electric field associated with a perturbation in a beam with the line charge density variation as

$$E_z(z,t) \cong -\frac{g}{4\pi\varepsilon_0\gamma^2}\frac{\partial\Lambda(z,t)}{\partial z}. \tag{4}$$

For a cylindrical, unbunched beam of radius a in a pipe of radius b the g-factor can be represented by the general, long-wavelength formula

$$g = 2\ln\frac{b}{a} + \alpha, \tag{5}$$

where α is a constant for which different values (1, 0.5, and 0) can be found in the literature. Neil and Sessler, in their original work [4], treated longitudinal instabilities of coasting beams in particle accelerators. They used a uniform-beam model with constant radius a, and derived the relation

$$\alpha = 1 - \left(\frac{r}{a}\right)^2, \tag{6}$$

with r being the radial position within the beam. This relation implies that the g-factor, as well as the field E_z, is a maximum with $\alpha=1$ on the axis, and reduces parabolically to a minimum with $\alpha=0$ on the beam surface with r=a. Averaging the field over the beam cross section yields $\alpha=0.5$. There is another model in unpublished papers which yielded $\alpha=0$ by assuming a constant volume charge density and perturbed beam radius. Hence, there is the question as to which value of α should be used. Further, the question also concerns some fundamental beam physics such as the correct model, the field distribution within the beams, surface wave or body wave, incompressibility of plasmas, etc.

We have developed a novel method to determine the parametric dependence of the g-factor associated with longitudinal perturbations in a beam [5]. In this technique, localized space-charge waves are launched on electron beams in a periodic solenoidal focusing channel and the propagation velocities of these waves are measured. At the same time, the beam radius a is independently measured by a phosphor screen plus CCD camera technique. This leads to an experimental determination of the parametric dependence of the geometry factor g on the radius a.

As shown in Fig. 1, the two localized space-charge waves move away from each other. The time interval between the two waves, which can be measured very accurately at different locations along the channel, is related to the traveling distance s by

$$\Delta t = \frac{2c_s}{v_0^2 - c_s^2} \cdot s \qquad (7)$$

Figure 4 plots the time interval of the two space-charge waves at five channel locations for two different phase advances σ_0. The beam energy is 5 keV and the beam current is 56 mA in this measurement. A least-square fitting of the experimental data yields $\Delta t/s$, and hence the wave velocity c_s according to Eq. (7); using this value of c_s one can determine the geometry factor g from Eq. (1).
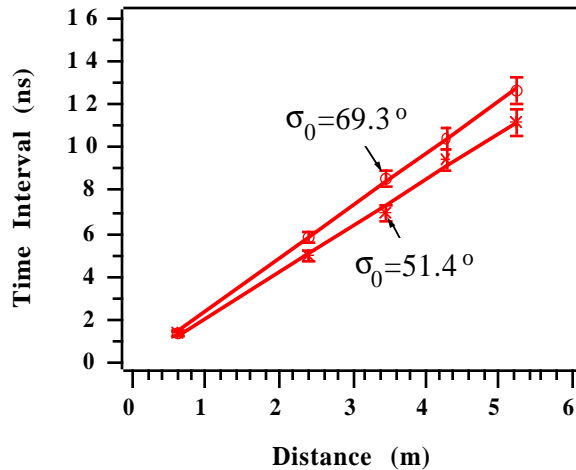

Fig. 4. Time interval between two space-charge waves vs. drifting distance for two different phase advances s_0, as measured by the five current monitors. The solid lines are least-square fitting of the experimental data.

The beam radius a is measured by the phosphor screen plus CCD camera technique. Using the two independent, experimental results for the g-factor and the beam radius a, we plotted the g-factor against the corresponding beam radius in the form of ln(b/a) for different experimental conditions as shown in Fig. 5. A least-square fitting of these data yields the relation of the g-factor as a function of the beam radius a, suggesting the correct formula for the g-factor is g=2ln(b/a), i.e. $\alpha=0$.
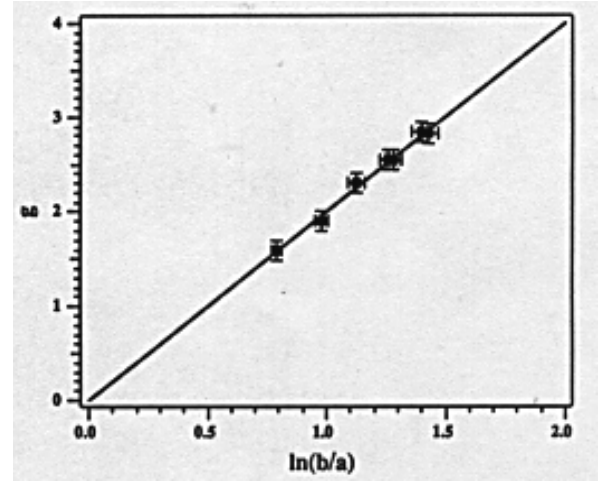

Fig. 5. The measured g-factor vs. ln(b/a). A least square fitting of the experimental data yields g≈2.01 ln(b/a)-0.01, suggesting the correct formula g=2 ln(b/a) as indicated by the solid line.

Our experimental result agrees with the model which assumes a constant volume density and perturbed beam radius. In space-charge dominated beams the perturbed electrical field within the beam is independent of the radial position. Though the volume charge density remains constant, the line charge density varies with perturbation due to the change of the beam radius. The perturbations do not compress the beam plasma density in this case. However, it is inappropriate to apply the surface wave concept since the perturbed field does penetrate through the whole medium.

IV. BUNCH END EFFECT ON SPACE-CHARGE WAVES

The effect of bunch ends on space-charge waves is important for the understanding and analysis of longitudinal instabilities in particle accelerators where perturbations often reach beam bunch ends. It is essential to know if the fast waves reflect off bunch front ends and become the slow waves, and vice versa. The previous studies on this subject included some theoretical work and computer simulations [6-9], showing the reflection off parabolic bunch ends, defined as the vanishing density points. We have conducted an experiment to study the end effect with an initially rectangular electron bunch [10]. The beam "end" here is referred to as the boundary between the flat region and the finite edge, quite different from the vanishing density point in previous work.

The experiment is performed in a similar way as in the generation of space-charge waves, and in the measurement of the geometry factor g. However, the initial perturbation is

placed very close to the bunch ends. The initial test is done with two waves launched close to the beam real end. The reflection of the slow waves is observed. In order to increase the signal to noise ratio, a single fast wave close to the beam front end is employed. Figures 6 (a-c) show the measured beam current signals from the first three fast wall-current monitors. Each figure contains three scope traces: the top one is the beam current waveform without perturbation, the middle one is the beam current at the same conditions except that the perturbation is added, the bottom one is the difference between those two signals and represents the net perturbation signal on the beam. The ordinate, which has a conversion factor of about 0.5 mA/mV (slightly different for each current monitor), is for the bottom traces only. The abscissa shows the relative time scale of the three wall-current monitor signals along the channel. In Fig. 6(a) the signals are from the first current monitor which is s=0.624 m from the electron gun. The beam energy is 5 keV, the average beam current is 52 mA, and the full width at half maximum (FWHM) of the pulse is 38.2 ns. The current perturbation signal has a total width of about 6 ns and an amplitude of 5.7 mA which is 11% of the beam current. The peak of the perturbation is about 3.5 ns away from the beam front "end", defined here as the turning point from the flat region to the rising edge, while the wave front of this wave packet is already very close to the beam front end. This is a single fast wave which would keep its shape as long as it stays in the flat region of the beam pulse. The second wall-current monitor at s=2.39 m sees two perturbation peaks separated by 6.2 ns, as shown in Fig. 6(b). This is caused by the splitting of the incident fast wave on the beam front end, which happens somewhere between the first and second current monitors. The peak on the left, i.e. the transmitted wave, has an amplitude of about 3.1 mA and has moved down the front edge, while the peak on the right, i.e. the reflected wave, has an amplitude of 2.3 mA and moves back towards the beam center. The sum of these two peaks is close to the single fast wave amplitude in Fig. 6(a). Figure 6(c) shows the signals from the third current monitor at s=3.48 m where the time interval between the two peaks has increased to 8.6 ns. The fourth and fifth current monitors see similar pictures with even larger separation times of the two peaks.

The propagation speed of space-charge waves can be measured with the beam current signals. For the reflected and transmitted waves in this experiment their speeds are measured with respect to the beam center which can be determined by the time-of-flight technique. The results are plotted in Fig. 7 where t=0 represents the beam center, the stars are for the reflected wave, and the dots are for the transmitted wave. For the reflected wave the least square fitting yields t (ns) = 13.0-1.46s (m), while for the transmitted wave t (ns) = 11.7+1.49s (m). The speed v of these two waves in the beam frame can be calculated from the relation

$$\left|\frac{dt}{ds}\right| = \frac{v}{(v_0 - v)v_0} , \qquad (8)$$

where v_0 is the beam center velocity in the lab frame. In this measurement the speed of the reflected wave is about 2.38 mm/ns, the speed of the transmitted wave is about 2.43 mm/ns.
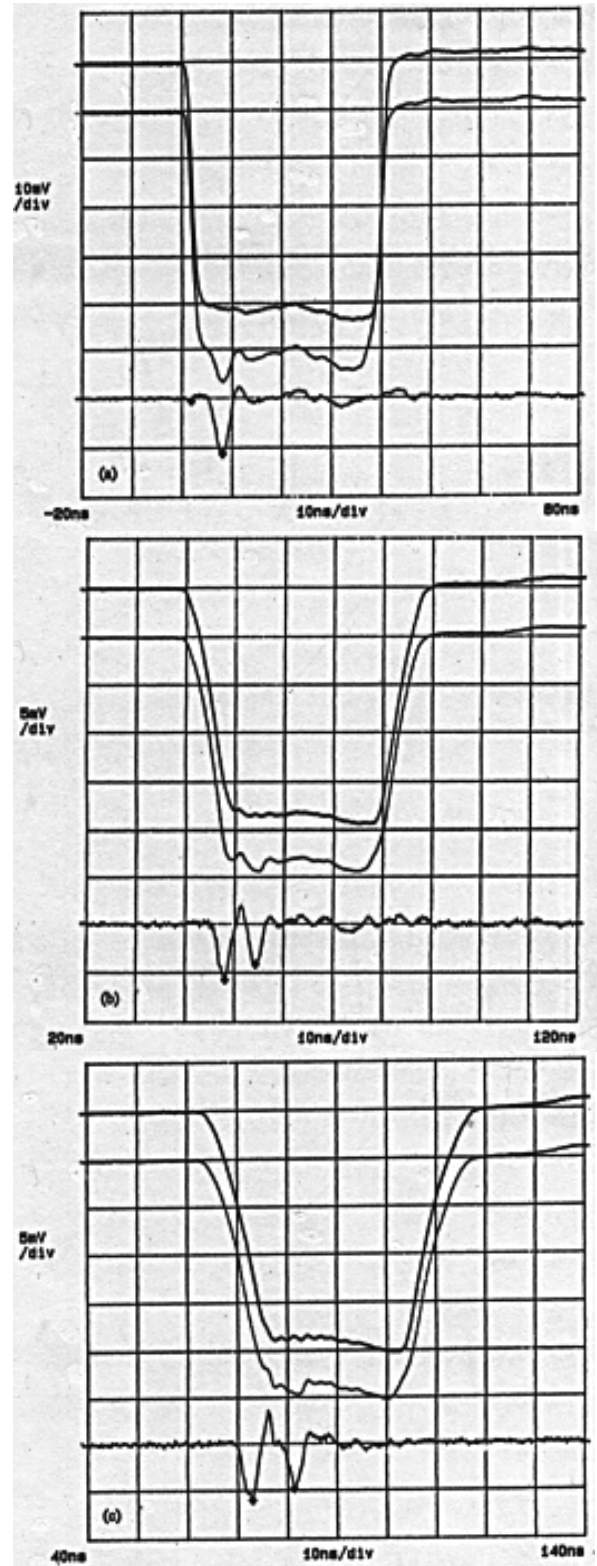

Fig. 6. Evolution of a fast wave around the beam front end:
(a) A single fast wave before reaching the beam front end, measured at s=0.624 m;
(b) Transmitted and reflected waves as measured at s=2.39 m;
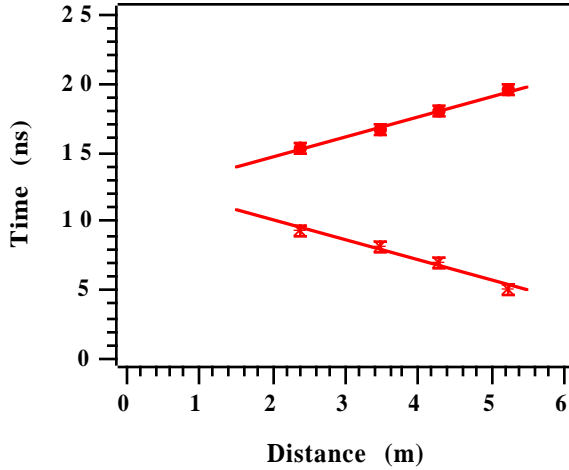(c) Transmitted and reflected waves as measured at s=3.48 m;

Fig. 7. Time interval between transmitted wave and beam center (dots), and between reflected wave and beam center (stars).

It is well known that an initially rectangular bunch suffers edge erosion due to the strong space-charge force at the beam edges [11, 12]. The top of both beam edges moves into the flat region with a speed c_S and the bottom of the edges moves outwards with a speed $2c_S$, where c_S is determined by Eq. (1). For space-charge dominated beams, c_S is a significant fraction of the beam center velocity v_0, and the edge erosion is very rapid. The experimental parameters yield the speed c_S of 2.30 mm/ns. In the calculation we use for the geometry factor the value $g=2\ln(b/a)=2.6$, determined in Section III. Thus, the three speeds, namely, the speed of the transmitted wave, the speed of the reflected wave and the beam edge erosion speed c_S have approximately the same values from this measurement.

A dynamic model based on beam impedance matching has been developed [10] and the analysis shows that under the condition

$$k >> \frac{2}{z_r} \quad , \quad \text{i.e.} \quad z_r >> \frac{\lambda}{\pi} \quad , \qquad (9)$$

where z_r is the beam edge length and λ is the perturbation wavelength, no reflection should occur. On the other hand, if the edge length z_r is negligibly smaller than λ/π, full reflection should occur. In the general situation between these two extremes, there should be partial reflection and partial transmission at the bunch end. The reflection coefficient can be calculated according to this model.

In the experiment the dependence of the reflected wave amplitude on the length of the front edge is qualitatively observed. When the initial perturbation is far away from the front end, the reflection is hardly seen in the experiment since the front edge is too long due to the edge erosion by the time the perturbation reaches the end. There is also experimental evidence showing that the amplitude of the reflected wave is significantly higher than the transmitted wave amplitude when the initial perturbation is very close to the front end so that the reflection happens with a short front edge.

V. BEAM DIAGNOSTICS WITH LOCALIZED SPACE-CHARGE WAVES

Through the study of the generation, propagation, and the bunch end effects of space-charge waves, a new beam diagnostic technique with localized perturbations has been developed [13]. Unlike the conventional approach with sinusoidal waves, a measurement of the propagation of localized space-charge waves in beam current or energy signals directly yields the propagation speed c_S of the perturbations according to Eq. (7). Thus, the geometry factor g can be calculated according to Eq. (1) after c_S is determined. For a space-charge dominated coasting beam the average beam radius can then be calculated by $g=2\ln(b/a)$. This provides a non-destructive method to diagnose beam size in high-current accelerators and transport channels. The measurement of the reflection of localized space-charge waves is demonstrated in Section IV. The other measurements with localized space-charge waves include the longitudinal space-charge wave impedance and longitudinal instability, etc. The details of this measurement is reported else where [14].

VI. REFERENCES

[1] J. D. Lawson, The Physics of Charged-Particle Beams, (Oxford University Press, New York, 1988), second edition, ch. 6.

[2] M. Reiser, Theory and Design of Charged Particle Beams, (John Wiley & Sons, Inc., edited by Mel Month, New York, 1994), ch. 6.

[3] J. G. Wang, D. X. Wang, and M. Reiser, Phys. Rev. Lett., **71**(12), 1836 (1993).

[4] V. K. Neil and A. M. Sessler, Rev. Sci. Instr. **36**(4), 429 (1965).

[5] J. G. Wang, H. Suk, D. X. Wang, and M. Reiser, Phys. Rev. Lett., **72**(13), 2029 (1994).

[6] E. P. Lee, in the Proceedings of the 1981 Linear Accelerator Conference, p. 263, Edited by R. A. Jameson and L. S. Taylor, Santa Fe, NM, Oct. 19-23, 1981.

[7] P. J. Channell, A. M. Sessler, and J. S. Wurtele, Appl. Phys. Lett., **39**(4), 15 August 1981.

[8] I. Hofmann, Z. Naturforsch, **37**a, 939 (1982).

[9] D. A. Callahan, A. B. Langdon, A. Friedman, and I. Haber, in the Proceedings of the 1993 Particle Accelerator Conference, Vol. 1, p. 730, Washington, D. C., May 17-20, 1993.

[10] J. G. Wang, D. X. Wang, H. Suk, and M. Reiser, Phys. Rev. Lett., **74**(16), pp. 3153-3156, April 17, 1995.

[11] A. Faltens, E. P. Lee, and S. S. Rosenblum, J. Appl. Phys., **61**(12), 5219 (1987).

[12] D. X. Wang, J. G. Wang, and M. Reiser, Phys. Rev. Lett., **73**(1), 66 (1994).

[13] J. G. Wang and M. Reiser, Rev. Sci. Instrum., **65**(11), 3444 (1994).

[14] H. Suk, J. G. Wang, and M. Reiser, in this proceedings.